Biochimica et Biophysica Acta 1808 (2011) 2136–2146

Contents lists available at ScienceDirect

Biochimica et Biophysica Acta

journal homepage: www.elsevier.com/locate/bbamem

The effect of aliphatic alcohols on fluid bilayers in unilamellar DOPC vesicles — A small-angle neutron scattering and molecular dynamics study

M. Klacsová [a,*], M. Bulacu [b], N. Kučerka [a,c], D. Uhríková [a], J. Teixeira [d], S.J. Marrink [b], P. Balgavý [a]

[a] Department of Physical Chemistry of Drugs, Faculty of Pharmacy, Comenius University, 832 32 Bratislava, Slovakia
[b] Groningen Biomolecular Sciences and Biotechnology Institute and Zernike Institute for Advanced Materials, University of Groningen, 9747 AG Groningen, The Netherlands
[c] Canadian Neutron Beam Centre, National Research Council, Chalk River, Ontario K0J 1J0, Canada
[d] Laboratoire Léon Brillouin (CEA/CNRS), CEA-Saclay, 911 91 Gif-sur-Yvette Cedex, France

ARTICLE INFO

Article history:
Received 21 December 2010
Received in revised form 30 March 2011
Accepted 21 April 2011
Available online 29 April 2011

Keywords:
Alcohol
Anesthetic
Lipid bilayer
Dioleoylphosphatidylcholine
Small-angle neutron scattering
Coarse-grained simulation

ABSTRACT

Small-angle neutron scattering and coarse-grained molecular dynamics simulations have been used to determine the structural parameters (bilayer thickness D, polar region thickness D_H, interfacial lateral area of the unit cell A_{UC} and alcohol partial interfacial area A_{CnOH}) of fluid dioleoylphosphatidylcholine:dioleoylphosphatidylserine (PCPS, DOPC:DOPS = 24.7 mol:mol) bilayers in extruded unilamellar vesicles with incorporated aliphatic alcohols (CnOH, n = 8–18 is the even number of carbons in alkyl chain). External $^2H_2O/H_2O$ contrast variation experiments revealed that D_H decreases as a function of alkyl chain length and CnOH:PCPS molar ratio. Using measurements at single 100% ^2H_2O contrast we found that (i) D decreases with CnOH:PCPS molar ratio and increases with CnOH chain length (at 0.4 molar ratio); (ii) A_{UC} significantly increases already in the presence of shortest CnOH studied (at 0.4 molar ratio), further increase is observed with longer CnOHs and at higher molar ratios; (iii) A_{CnOH} of alcohol molecules in PCPS bilayer increases linearly with the alkyl chain length, A_{CnOH} obtained for CnOHs with $n \leq 10$ corresponds to $A_{CnOH} \leq 20 Å^2$ — a value specific for the crystalline or solid rotator phase of alkanes. All these structural modifications induced by studied CnOHs were reproduced in MD simulations. The computational results give an accurate description of the alcohol effects at the molecular level, explaining the experimental data. The anomaly in A_{CnOH} is discussed via the "umbrella" effect described for cholesterol.

© 2011 Elsevier B.V. All rights reserved.

1. Introduction

Thanks to their general anesthetic potency, alcohols are widely used in studies concerning the mechanism of anesthesia. The general anesthetic potency of primary aliphatic alcohols CnOH increases up to C11OH and then decreases, compounds longer than C13OH are non-anesthetic, i.e. the homologous CnOH series displays a cut-off in the anesthetic potency [1,2]. The partition coefficient of CnOH between the lipid bilayer and the aqueous phase increases exponentially with the CnOH chain length n also in the region of cut-off [3], the cut-off effect is therefore an exception to the Meyer–Overton rule, according to which the anesthetic potency should increase with the lipophility. This exception is frequently used as an indication that alcohols act by binding directly to sensitive target proteins, and not via their action on the lipid bilayer part of membranes. However, cut-off type dependencies are observed also in biocidal potencies of CnOHs, e.g. in the lethal activity against minnows [4] and bacteria [5,6], growth impairment in ciliate protozoan [7] and in the lethal action against 1st instar mosquito larvae [8]. An important pharmaceutical application of CnOHs is their use as penetration enhancers in transdermal drug delivery. Similarly to the effects earlier, the permeation enhancing effect increases with increasing chain length up to C10OH and decreases for alcohols with longer chains [9,10]. The absorbance of bacteriorhodopsin in the purple membrane of *Halobacteria* is influenced by CnOH with the maximum effect at C11OH–C13OH [11].

It is not excluded that some of the aforementioned effects can be caused directly or indirectly by dissolving of alcohol molecules in the lipid part of biomembranes and this is why interactions of alcohols with lipid bilayers and monolayers are widely studied. ^{2}H NMR studies concerning the effect of alcohols on structural properties of fluid DMPC bilayers revealed that C4OH decreases the ordering of the bilayers, unlike C8OH which has the opposite effect and longer chain alcohols which have little effect ([12] and references therein). The chain-length-dependent effect of alcohols on EYPC and DPPC bilayers was observed in a fluorescent probe study: C5OH disordered the

Abbreviations: PC, phosphatidylcholine; DOPC, 1,2-dioleoyl-*sn*-glycero-3-phosphatidylcholine; DOPS, 1,2-dioleoyl-*sn*-glycero-3-phosphatidylserine; DMPC, 1,2-dimyristoyl-*sn*-glycero-3-phosphatidylcholine; DPPC, 1,2-dipalmitoyl-*sn*-glycero-3-phosphatidylcholine; PCPS, homogeneous mixture of DOPC (96 wt.%) and DOPS (4 wt.%); CnOH, alkan-1-ol (n is the number of carbons in the aliphatic chain); EYPC, egg yolk phosphatidylcholine; SANS, small-angle neutron scattering; SAND, small-angle neutron diffraction; SAXS, small-angle X-ray scattering; SAXD, small-angle X-ray diffraction; WAXD, wide-angle X-ray diffraction; GIXD, grazing incidence X-ray diffraction; MD, molecular dynamics; ULV, unilamellar vesicle

* Corresponding author. Tel.: +421 2 50117 289; fax: +421 2 50117 100.
E-mail address: klacsova@fpharm.uniba.sk (M. Klacsová).

0005-2736/$ – see front matter © 2011 Elsevier B.V. All rights reserved.
doi:10.1016/j.bbamem.2011.04.010

membrane at all depths but was more effective in the bilayer center than closer to the polar headgroups, C14OH was accommodated into the membrane without effect or with increased order and the effects of C10OH were intermediate between C5OH and C14OH [13]. In fluid SOPC bilayers, the insertion of short chain alcohols (C1OH–C4OH) results in the chain-length-dependent interfacial tension reduction with concomitant chain-length-dependent reduction in mechanical moduli and increase of area per SOPC molecule as observed by micropipette aspiration technique [14]. While the results of MD simulations suggest that insertion of short chain alcohol (C2OH) into fluid DMPC bilayers should increase the area per lipid and decrease the bilayer thickness and the ordering of the lipid, the long chain alcohols (C8OH, C10OH, and C14OH) should have opposite effects [15]. The Raman lateral chain order in DPPC bilayers is increased by C8OH and C18OH in the fluid lamellar phase, while C8OH decreases and C18OH increases this order in the gel phase ([16], and J. Cirák — personal communication). Although the effects of alcohols on structural and thermodynamic properties of the bilayers are small at clinical concentrations [17], the bilayer lateral pressure profile can change significantly also at these concentrations. Results of lattice statistical thermodynamic calculations indicate that the incorporation of alcohols into a lipid bilayer selectively increases the lateral pressure near the aqueous interfaces and compensatively decreases it toward the center of the bilayer, moreover, a qualitative agreement with the anesthetic potency including the cut-off effect was observed [18,19].

In the literature, the effects of short chain alcohols on the structure of DMPC, DPPC and DSPC bilayers are well documented [20,21]. However, direct experimental data involving long chain alcohols are scarce and contradictory. Pope et al. [22] have found using SAXD that the increase of C8OH concentration in fluid DMPC lamellar phase results in the increase of surface area per DMPC molecule at the bilayer/water interface while the DMPC bilayer thickness remains approximately constant. On the other hand, the recent SAND study of the fluid DOPC lamellar phase indicates an increase in the surface area per DOPC in the presence of CnOH (n = 8–18), accompanied by a decrease in the bilayer thickness [23]. However, these diffraction experiments were done at relatively low hydrations, at 10 mol of water per mol of DMPC in [22] and at 14-20 mol of water per mol of DOPC in [23], which might modulate alcohol effects. To the best of our knowledge, the only study at physiologically relevant high bilayer hydration is the SANS on DMPC ULVs in excess heavy water (P. Westh, personal communication): C6OH decreases the thickness of the fluid bilayer while C12OH increases it; the effect of C8OH is intermediate between these two, slightly decreasing the bilayer thickness.

Evidently, structural data for long chain alcohols are needed, especially in relation to lipid mechanisms of the cut-off which is observed at C10OH–C13OH as summarized earlier. We have therefore chosen to study the effects of long aliphatic alcohols, from C8OH to C18OH, on structural parameters of fluid bilayers in unilamellar PCPS vesicles. Unsaturated phospholipids are important constituents of biological membranes and due to their low transition temperature they are conveniently used as models of fluid bilayers in biological membranes, and unilamellar vesicles are topologically similar to cell membranes. We prepare unilamellar vesicles by extrusion. The small amount of DOPS present in DOPC bilayers charges the bilayer surface negatively and thus prevents oligolamellar vesicle formation during extrusion and vesicle aggregation after extrusion, while it does not affect the structure of DOPC bilayer itself [24]. Using SANS on unilamellar vesicles, we obtain the bilayer thickness, D, the bilayer polar region thickness, D_H, and the bilayer hydrophobic region thickness, $D_C = D - 2D_H$, the lateral area of the unit cell consisting of a phospholipid molecule and a particular fraction of the alcohol at the bilayer–aqueous phase interface, A_{UC}, and the number of water molecules per one phospholipid located inside the headgroup region, N_W. Effects of alcohols on the transversal and lateral thermal expansivities of the bilayer are evaluated from the temperature dependencies of D and A_{UC}, respectively. The trends of D and A_{UC} observed experimentally are reproduced in coarse-grained molecular dynamics simulations of fully hydrated phosphatidylcholine bilayers with CnOH molecules inserted. The simulations provide additional insight from the molecular level of the alcohol effects on the bilayer.

2. Materials and methods

2.1. Materials

Synthetic DOPC and DOPS were purchased from Avanti Polar Lipids (Alabaster, USA) and used as received. CnOHs (n = 8–18 is the even number of carbons in the aliphatic chain) with 99% purity were purchased from Sigma (St. Luis, USA). The organic solvents of spectral purity were obtained from Slavus (Bratislava, Slovakia). Solvents were redistilled before use. Heavy water (99.96% ^2H_2O) was obtained from Merck (Darmstadt, Germany).

2.2. Contrast variation samples

Required amounts of DOPC, DOPS and CnOH were weighted into a glass tube and mixed in a methanol-chloroform solution. The solvent was then evaporated under a stream of gaseous nitrogen and its traces removed by an oil vacuum pump. To prevent evaporation of CnOHs, samples were cooled down to −15 °C during evacuation. The amount of dried sample was checked gravimetrically. Samples were hydrated with heavy water and homogenized by vigorous vortex mixing. Obtained stock dispersions were extruded 51 times through 200 nm, thereafter 51 times through 50 nm pores in carbohydrate filters (Nuclepore, USA) using LiposoFast Basic extruder (Avestin, Canada). Samples were prepared in Eppendorf plastic tubes using 0.5 ml of extruded stock dispersion and additional H_2O and/or heavy water to reach total volume 1 ml and required $^2H_2O/H_2O$ contrast (100, 90, 80, 70, 60 and 50% heavy water). The final lipid concentration was 10 mg/ml. The concentration of CnOH in PCPS (DOPC:DOPS = 24.7 mol:mol) bilayers was calculated using the CnOH partition coefficients published in [3,25,26].

2.3. Samples in heavy water

Stock solutions of DOPC, DOPS and CnOHs, respectively, were prepared in methanol-chloroform mixture. The required amount of lipid solution (10 mg lipid/sample) and appropriate amount of CnOH were transferred into particular glass tubes. The solvent was removed as described earlier. Dried samples were dispersed in heavy water. Samples were homogenized by vigorous vortex mixing and extruded shortly before SANS experiment as described earlier. The correction for CnOH partition between aqueous phase and PCPS bilayers was done using the partition coefficients from [3,25,26].

2.4. SANS experiment

SANS measurements were performed at the PAXE spectrometer located at the extremity of the guide G5 (cold source) of the Orphée reactor at LLB Saclay [27]. The spectrometer was equipped with the xy position sensitive detector. The scattering data were acquired at two positions of the detector, corresponding to sample–detector distance 1.3 m and 5.05 m, respectively. The wavelength of neutrons was $\lambda = 0.6$ nm. The samples were poured into quartz cells (Hellma, Germany) to provide 1 or 2 mm sample thickness. The sample temperature was set and controlled electronically to ± 1 °C. The acquisition time for samples prepared in heavy water was 30 min, for samples with heavy water contents 90, 80, 70, 60 and 50% it was 45, 60, 90, 105 and 120 min, respectively. The normalized SANS intensity $I(q)$ as a function of the scattering vector modulus q was obtained as described in detail previously [28].

2.5. SANS data evaluation

The experimental normalized SANS intensity $I(q)$ as a function of the scattering vector modulus q was evaluated as described extensively earlier [29,30]. It is supposed that extruded ULVs are polydisperse hollow spheres with the single bilayer separating the inside and outside aqueous compartments, and that the bilayer can be divided into three strips corresponding to two polar headgroup regions (one on each side of the bilayer) and the bilayer center spanning hydrocarbon region. The radii of strips are then as follows: R_0 — the inner radius of the bilayer and the inner radius of the inner polar strip, $R_1 = R_0 + D_H$ — the outer radius of the inner polar strip and the inner radius of the central hydrophobic strip, $R_2 = R_1 + D_C = R_0 + D_H + D_C$ — the outer radius of the central hydrophobic strip and the inner radius of the outer polar strip, and the outer radius of the outer polar strip equal to the outer vesicle radius $R = R_3 = R_2 + D_H = R_0 + 2D_H + D_C = R_0 + D_L$. It is supposed further that the polydispersity of ULVs can be described by the Schulz distribution function, $G(R)$, of vesicle radii R. The theoretical SANS intensity $I_{theor}(q)$ of such polydisperse ULVs is

$$I_{theor}(q) = N_P \int_{q'} T(q') \int_R G(R) I(R, q-q') dR dq' \quad (1)$$

where N_P is the number density of particles, $T(q)$ is the SANS spectrometer resolution function and $I(R, q-q')$ the structure factor of the vesicle with radius R. The structure factor is the square of form factor $F(q)$ which is for the 3-strip model given by

$$F(q) = \frac{4\pi}{q^3} \sum_{i=1}^{3} \Delta\rho_i \{[qR_i \cos(qR_i) - \sin qR_i] - [qR_{i-1} \cos(qR_{i-1}) - \sin qR_{i-1}]\} \quad (2)$$

where $\Delta\rho_i(r)$ is the neutron scattering length density contrast of the i-th strip against the aqueous phase. The polar strip contrast against the aqueous phase is

$$\Delta\rho_H = \frac{n_{PCPS}B_H + n_{CnOH}B_{OH} + n_W B_W}{n_{PCPS}V_H + n_{CnOH}V_{OH} + n_W V_W} - \rho_W \quad (3)$$

where n_{PCPS}, n_{CnOH} and n_W is the number of PCPS, alcohol and water molecules, respectively, located in the PCPS bilayer; V is the volume and B the coherent scattering length, and subscripts H, OH and W abbreviate PCPS headgroup, alcohol OH group and water, respectively; ρ_W is the neutron scattering length density of aqueous phase. The contrast of the bilayer hydrophobic strip against the aqueous phase is

$$\Delta\rho_C = \frac{n_{PCPS}B_C + n_{CnOH}B_{Cn}}{n_{PCPS}V_C + n_{CnOH}V_{Cn}} - \rho_W \quad (4)$$

where the volume of PCPS and CnOH hydrocarbon part is $V_C = V_{PCPS} - V_H$ and $V_{Cn} = V_{CnOH} - V_{OH}$, respectively, B_C and B_{Cn} are the corresponding coherent scattering lengths, and V_{PCPS} and V_{CnOH} are the PCPS and CnOH molecular volumes. It is evident from Eqs. (3) and (4), that water molecules are assumed to penetrate the polar strip only and that we treat PCPS as a single molecule, i.e. the weighted average value of scattering lengths is used. The PCPS headgroup volume ($V_H = 321$ Å^3) was calculated accordingly from the densitometric data in [31] and was used as invariant with temperature. Furthermore, we suppose that the CnOH hydroxyl groups and some water molecules are located in the polar strips. The hydrophobic volumes V_C and V_{Cn} were calculated using the methine, methylene and methyl group volumes. The volumes of CH and CH_2 groups were taken from Uhríková et al. [32], the volume of the CH_3 group was calculated using the known lipid chain volume [31]. The volume of OH group of CnOHs located in the bilayer was determined previously by densitometry [31]. All component volumes were recalculated for particular temperatures using the thermal volume expansivities from [31]. The volume of water molecule was calculated as a weighted average of H_2O and ^2H_2O molecular volumes at given temperature [33] according to the sample contrast. The coherent scattering lengths were calculated using the known neutron coherent scattering lengths of nuclei [34]. Defining $N_W = n_W/n_{PCPS}$, it is evident that

$$A_{UC} = \frac{V_H + N_W V_W + \frac{n_{CnOH}}{n_{PCPS}} V_{OH}}{D_H} = \frac{2\left(V_C + \frac{n_{CnOH}}{n_{PCPS}} V_{Cn}\right)}{D_C} \quad (5)$$

This equation provides a constraint between the three bilayer structural parameters D_H, D_C, and N_W reducing the number of independent parameters to two. These structural parameters are obtained by the iterative fitting approach that results in the bilayer scattering length density profile. The experimentally obtained scattering curves $I(q)$ are fitted with those calculated theoretically $I_{theor}(q)$ plus the q-independent constant background I_b, using the function minimization and error analysis program Minuit (CERN Program Library entry D506). During the fitting, the D_H value is usually constrained in case of $I(q)$ data obtained with samples at a single contrast. However, this constrain is not needed when the sample is measured at several $^2H_2O/H_2O$ compositions and all SANS curves obtained are fitted simultaneously. The mean vesicle radius and vesicle size polydispersity are also obtained in the fitting, but these will not be discussed in the present work, because the bilayer local structure is the subject of most interest. For more details about the fitting procedure and for further references see recent papers of our group [29,30].

Using data from thermal measurements, the transversal (α_D) and lateral (α_A) coefficients of isobaric thermal expansivity of the PCPS + CnOH bilayers determined by equations

$$\alpha_D = \frac{1}{D}\left(\frac{\partial D}{\partial T}\right)_P \quad (6)$$

$$\alpha_A = \frac{1}{A_{UC}}\left(\frac{\partial A_{UC}}{\partial T}\right)_P \quad (7)$$

where T is the absolute temperature, were obtained by the nonlinear least squares fitting of the experimental data in the temperature range 20–51 °C.

Finally, we should like to note that the bilayer structural parameters are best obtained when employing several techniques simultaneously, as was recently demonstrated using a simultaneous analysis of SANS and SAXS data inspired by MD simulations [35]. Any partial data analysis, including that in the present paper, may provide biased absolute values of parameters. However, qualitative trends obtained from such results can be readily detected.

2.6. MD simulations

To characterize the structural changes induced in the bilayers by long aliphatic alcohols, we have simulated a fully hydrated phosphatidylcholine (PC) bilayer incorporating CnOHs at different concentrations and with variable chain lengths n = 8, 12, 16. All simulations described in this paper were carried out with the GROMACS molecular dynamics package [36], using the MARTINI coarse-grained force field [37]. This coarse-grained representation is known to accurately reproduce the structural and dynamic properties of many lipids in the lamellar fluid state [35,37,38]. It has been also recently used to study the effects of short alcohols [39] or lysolipids [40] incorporated in DPPC bilayers, while a very similar coarse-grained representation was successful in reproducing the phase diagram of a DSPC bilayer containing short alcohols [41].

Each individual PC lipid consists of five types of coarse-grained particles: two hydrophilic (type "Q_0" and "Q_a" modeling the choline

and the phosphate moiety); two intermediately hydrophobic (type "N_a" for the glycerol); and ten hydrophobic particles (type "C_1" and "C_3") representing the two chains with 18 carbon units each. The less hydrophobic "C_3" type is used to model the unsaturated bond. Since the C1 and C3 coarse-grained particles are built to represent four carbon units, the length of the PC tails is slightly longer in our model than those of DOPC at atomistic scale. The alcohols are represented by a polar "P_1" head particle and one / two / three "C_1" particles for the chains of the octanol / dodecanol / hexadecanol, respectively. The solvent is modeled by hydrophilic particles (type "P_4") each representing four real water molecules. All these coarse-grained particles interact via Lennard–Jones (LJ) potential with different well depth parameters depending on a specific pair type. The electrostatic interaction between choline (charge +1e) and phosphate (charge −1e) particles is modeled by a screened Coulomb potential, while the connectivity and stiffness of the molecules are modeled by a set of elastic bonds and harmonic bending potentials. For explicit details of the interaction parameters we refer the reader to the original publications [37,38] or to the web-site http://cgmartini.nl.

To create the starting configuration of the membrane with inserted alcohols, a number of randomly chosen lipids from a pure PC bilayer have been converted to alcohols. In all cases the same hydration level (16 coarse-grained water particles per lipid) was kept. For instance, a membrane with C16OH at CnOH: PC = 0.4 molar ratio consists of 5688 coarse-grained particles: 180 PC lipids, 72 C16OH molecules and 2880 coarse-grained water particles. Periodic boundary conditions in all directions have been employed. The bilayer, the alcohols and the water were independently coupled to a heat bath of T = 293 K (time constant $\tau_t = 1$ ps) while the system pressure was scaled semi-isotropically to P = 1 bar both in the plane of the bilayer and perpendicular to the bilayer (time constant $\tau_P = 1$ ps and compressibility $\beta = 4.5 \times 10^{-5}$ bar^{-1}) [42]. The systems were simulated with a time step of 160 fs. After equilibration, a production run of 20 microseconds has been used for the analysis. The time reported in this paper is the effective time that accounts for the speeded-up dynamics specific to coarse-grained simulations (the effective time equals four times the actual simulation time [37]).

As a straightforward characterization of the lipid bilayers we have computed the area per lipid (A), the alcohol partial interfacial area (A_A), and bilayer thickness parameter (D_{PP}) for different alcohol concentrations and alcohol chain lengths. The notations A_{UC}, A_{CnOH} and D have been changed to better differentiate between the MD and the experimental results. A was measured as the area of the simulation box in the direction parallel to the bilayer plane, divided by the number of the lipids per monolayer. In the assumption that all the alcohol molecules are equally distributed in the monolayers, we have estimated the A_A as

$$A_A = \frac{n_{DOPC}}{n_{CnOH}}(A - A_{DOPC}) \tag{8}$$

D_{PP} was calculated as the distance between the two peaks in the distribution of the phosphate groups along the direction perpendicular to the bilayer. To characterize the relative orientation of the lipid chains inside the bilayer we have computed the uniaxial order parameter S for all the bonds between the coarse-grained chain particles:

$$S = \frac{1}{2}\left\langle 3\cos^2\theta - 1\right\rangle \tag{9}$$

where θ is the angle between the membrane normal and each individual bond. The averaging is done over all lipid chains and over time. Perfect parallel alignment is indicated by $S = 1$, perfect perpendicular alignment by $S = -0.5$ while a random orientation is characterized by $S = 0$.

3. Results and discussion

In the present work, we study several series of samples at several temperatures. Most of these samples were prepared at a single bilayer-aqueous phase contrast (in heavy water) and at a single n_{CnOH}:n_{PCPS} = 0.4 molar ratio, mainly because of shortage of neutron beam time. The n_{CnOH}:n_{PCPC} = 0.4 molar ratio was selected because our previous diffraction [23] and volumetric [31] experiments indicated a phase separation at n_{C16OH}:n_{PCPS} > 0.5 molar ratio. For evaluation of SANS data obtained at the single contrast, the value of polar region thickness, D_H, must be constrained as mentioned earlier. First experiments were therefore aimed to find whether the D_H is dependent or not on the presence of CnOH. Consequently, pure PCPS vesicles and PCPS vesicles with the addition of C10OH and C16OH at n_{CnOH}:n_{PCPS} = 0.4 molar ratio were studied at six different $^2H_2O/H_2O$ aqueous phase compositions (100, 90, 80, 70, 60 and 50% of heavy water) at 20 °C. Selected experimental SANS data are shown in Fig. 1. The Kratky–Porod plots of $\ln[I(q)q^2]$ vs. q^2 in the Guinier range of q were linear (not shown) indicating scattering on ULVs; the absence of any correlation peak in Kratky–Porod plots as well as in Fig. 1 is, therefore, an evidence that the prepared vesicles were unilamellar and did not contain an appreciable amount of paucilamellar or multilamellar vesicles, which could complicate further analysis. The absence of any correlation peak further confirms that the intervesicular interactions are negligible at the lipid concentrations and vesicle sizes used, in agreement with [24,43]. The SANS data points for each sample and each contrast were obtained at two different detector positions; the data from these positions partially overlap in the region 0.04 Å$^{-1} \le q \le$ 0.06 Å^{-1}. The small difference between these two data point sets is caused by different SANS spectrometer resolution functions at two different detector positions.

3.1. Bilayer polar region thickness

The SANS data were evaluated using the strip-model of the lipid bilayer as described earlier by the simultaneous fitting of experimental $I(q)$ data obtained for one sample at all $^2H_2O/H_2O$ aqueous phase compositions. The best fits are shown in Fig. 1 by solid curves. The bilayer thickness D, the lateral area A_{UC} of the unit cell consisting of a phospholipid PCPS "molecule" and a particular fraction of alcohol, and the number of water molecules N_W per one PCPS molecule located inside the polar headgroup region determined in the fits will be discussed later. The headgroup volume V_H needed for fitting is not known precisely. For example, the experimental values for phosphatidylcholines span the range from 319 Å^3 for DPPC at 24 °C [44] to 331 Å^3 for DMPC at 10 °C [45], in solid-like bilayers in gel $L_{\beta'}$ phase. Pabst et al. [46] note that "… the headgroup conformation is likely to depend on temperature, pressure, chain tilt …, or hydration …, which directly affects the headgroup dimensions, so that the volume of the PC headgroup in the $L_{\beta'}$ phase is not evidently the same as in the L_α phase. Hence a method which utilizes the assumption of a constant headgroup volume and size, respectively, and even relies on measurements of systems different from the situation of fully hydrated bilayers, can be justifiable, but certainly leads to a rough estimate…". In the previous paper from our group [32], it was found that the V_H value changes by less than 0.2% within the range of 20–40 °C in fluid bilayers of monounsaturated diacylphosphatidylcholines, so the temperature effects can be neglected. Therefore, we use the value V_H = 321 Å^3 obtained from our densitometric data for PCPS "molecule" [31] if not indicated otherwise. Nevertheless, to check the effect of headgroup volume on the polar region thickness D_H, we have refitted the contrast variation data for different headgroup volumes. The changes were relatively small — $D_H = 9.93 \pm 0.05$ Å for V_H = 319 Å^3, $D_H = 9.97 \pm 0.05$ Å for V_H = 331 Å^3 and $D_H = 9.94 \pm 0.05$ Å for our preferred value V_H = 321 Å^3 in case of control PCPS vesicles without CnOH. This is in agreement with the datum $D_H = 9.0 \pm 1.2$ Å extracted by Pabst et al. [46] from inner and outer contrast variation SAND data obtained with oriented DPPC bilayers at low hydration [47,48].

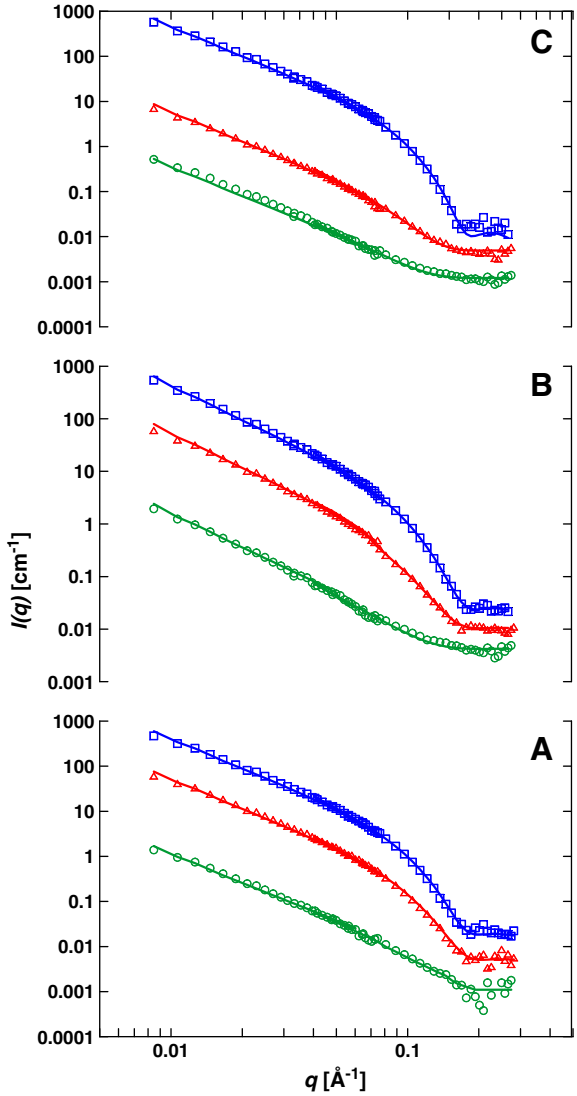

Fig. 1. Experimental SANS curves obtained for PCPS (A), C10OH + PCPS (B) and C16OH + PCPS (C) vesicles at 100% (□), 70% (△) and 50% (○) $^2H_2O/H_2O$ contrasts at n_{CnOH}:n_{PCPS} = 0.4 molar ratio and 20 °C. Scattering curves are shifted vertically for clarity of presentation. Solid lines correspond to the best fits as obtained using the model described in Materials and methods.

The most crucial finding from our outer contrast variation experiments is that the polar region thickness of the PCPS bilayer slightly decreases after incorporation of CnOH molecules and that this decrease is a function of CnOH chain length, i.e. with increasing n the thickness D_H decreases. Based on this finding and on assumptions that D_H decreases linearly with increasing concentration of C10OH and C16OH and with n, we have calculated the PCPS polar region thickness for the other alcohols studied (Table 1) as well as for different n_{CnOH}:n_{PCPS} molar ratios (not shown). In the following evaluation, we use these D_H values as fixed parameters. However, we should like to emphasize that qualitatively similar D, A_{UC} and N_W dependencies on CnOH chain length n and on n_{CnOH}:n_{PCPS} molar ratio as reported later were obtained when the polar region thickness was fixed to D_H = 9.0 Å or to D_H = 10.0 Å.

3.2. Bilayer thickness and surface area

Structural parameters of PCPS bilayers with intercalated alcohols, as obtained by fitting of experimental data from samples prepared at a single contrast (in heavy water) are displayed in Figs. 2, 3 and 4. For comparison, the data from contrast variation experiments are included in Fig. 4. The bilayer thickness D = 50.0 ± 0.3 Å and D = 49.5 ± 0.2 Å was obtained for the PCPS control samples in heavy water and in contrast variation series, respectively, both at 20 °C and with V_H = 321 Å^3 fixed. The variation in the headgroup volume from V_H = 331 Å^3 to V_H = 319 Å^3 changed these results of fitting by less than 0.6%, which is within the error margins of D obtained. For pure DOPC ULVs at 30 °C the value D = 49.0 ± 0.8 Å was observed in [29] using SANS. The hydrophobic region thickness of DOPC bilayers found in [35] using a much more involved simultaneous analysis of SANS and SAXS data inspired by MD simulations is D_C = 29.0 ± 0.6 Å at 30 °C. To compare the thickness values at the same temperature, we adjusted the PCPS data for transversal thermal expansivity (see Eq. (6) and Fig. 5) and obtained D = 49.4 ± 0.3 Å and D = 48.9 ± 0.2 Å at 30 °C for heavy water and contrast variation samples, respectively, corresponding to D_C = 29.5 ± 0.4 Å and D_C = 29.0 ± 0.3 Å, respectively, when using the D_H value found for PCPS (Table 1). It is evident from these comparisons that the PCPS data coincide with the DOPC data in [29] and [35] within error margins, i.e. the small amount of DOPS in bilayers influences the bilayer thickness negligibly.

The bilayer thickness was found to decrease with increasing CnOH molar ratio n_{CnOH}:n_{PCPS} in bilayers for all alcohols studied (C8OH and C16OH — Fig. 2, C12OH — Fig. 3). At the constant n_{CnOH}:n_{PCPS} = 0.4 molar ratio, the bilayer thickness increases with increasing CnOH chain length n reaching for C16OH and C18OH the D value of the pure PCPS lipid system within the experimental error (Fig. 4). The results of contrast variation experiments fit well this dependence. The CnOH effect on the bilayer thickness can be explained simply by the mismatch between CnOH and PCPS hydrocarbon chain lengths — the intercalation of shorter alcohols into a lipid bilayer induces voids under their terminal methyl groups and these voids are filled-in with neighboring lipid acyl chains, what leads to a decrease in bilayer thickness. When longer alcohols are intercalated at the same bilayer concentration, their alkyl chains penetrate more deeply into the hydrophobic region and the change in bilayer thickness is smaller. Obviously, the actual change of thickness is dependent on the bilayer surface area.

The lateral area of the unit cell A_{UC} at the bilayer–water interface, in the case of control sample without CnOH, is the molecular area of PCPS of control sample without CnOH, A_{PCPS}. From the SANS data of PCPS vesicles in heavy water we evaluated A_{PCPS} = 64.6 ± 0.7 Å^2 at 20 °C when our preferred value V_H = 321 Å^3 for PCPS was used; the variation in the headgroup volume from V_H = 331 Å^3 to V_H = 319 Å^3 changed this value by less than 1.4%. The molecular area of DOPC at 30 °C found by Kučerka et al. [35] using the simultaneous SANS and SAXS data evaluation is A_{DOPC} = 66.9 ± 1.0 Å^2. Extrapolating this datum to 20 °C by using the lateral thermal expansivity coefficient α_A = 0.0029 K^{-1} (see [49] and Eq. (7)), the value A_{DOPC} = 65.0 ± 1.0 Å^2 is obtained, in excellent agreement with A_{PCPS} at this temperature. It is seen from this comparison that the presence of DOPS in our

Table 1
Bilayer polar region thickness D_H of the PCPS bilayers in unilamellar vesicles without and with alcohols of different chain length at n_{CnOH}:n_{PCPS} = 0.4 molar ratio at 20 °C. ♥ — obtained by fitting of contrast variation data, * — extrapolated data.

Bilayer	PCPS	PCPS + C8OH	PCPS + C10OH	PCPS + C12OH	PCPS + C14OH	PCPS + C16OH	PCPS + C18OH
D_H (Å)	9.94 ± 0.05♥	9.40*	9.35 ± 0.05♥	9.30*	9.25*	9.20 ± 0.05♥	9.15*

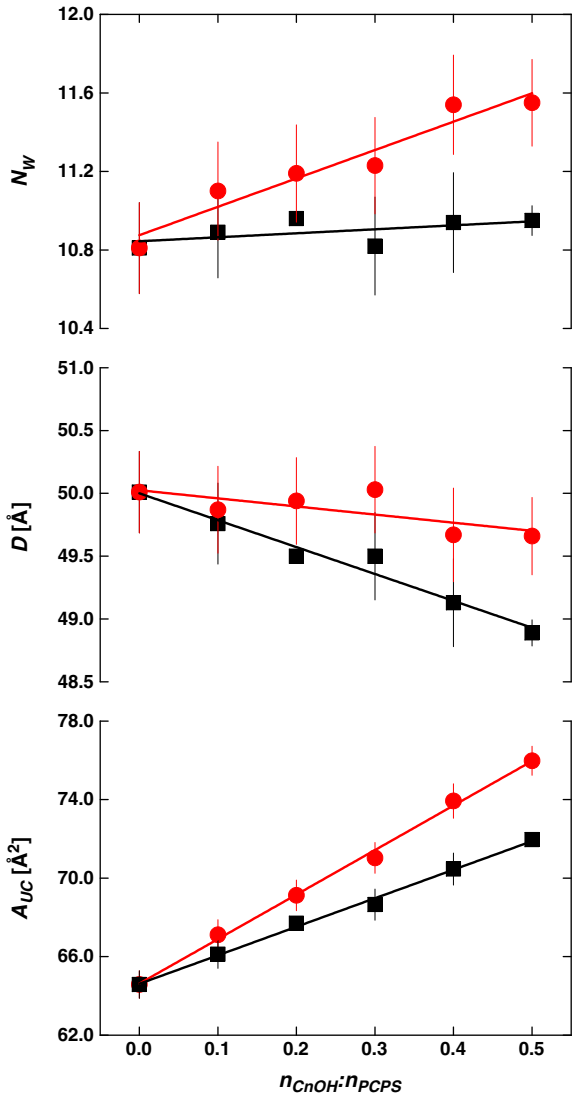

Fig. 2. Lateral area of the unit cell (A_{UC}), bilayer thickness (D) and number of water molecules per PCPS "molecule" (N_W) as a function of n_{CnOH}:n_{PCPS} molar ratio in PCPS + CnOH bilayers at 20 °C; n = 8 (■), 16 (●).

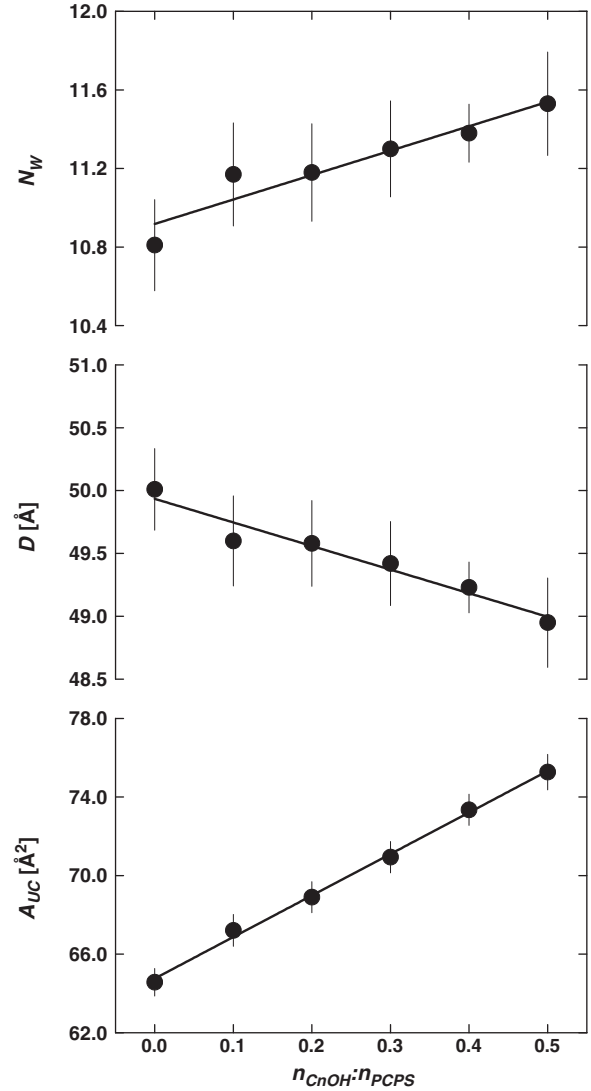

Fig. 3. Lateral area of the unit cell (A_{UC}), bilayer thickness (D) and number of water molecules per PCPS "molecule" (N_W) as a function of n_{C12OH}:n_{PCPS} molar ratio in PCPS + C12OH bilayers at 20 °C.

samples is too low to influence the interfacial molecular area significantly, though the interfacial area of DOPS is smaller by about 7.2 Å^2 than that of DOPC [50].

The lateral area of the unit cell A_{UC} was found to increase with increasing CnOH molar ratio n_{CnOH}:n_{PCPS} in bilayers (C8OH and C16OH — Fig. 2, C12OH — Fig. 3). The steepness of the A_{UC} increase differs between alcohols, where larger increase is found for longer CnOH chain lengths (C16OH>C12OH>C8OH). The lateral area A_{UC} raises significantly at a constant n_{CnOH}:n_{PCPS} = 0.4 molar ratio and 20 °C, in comparison with pure PCPS bilayers, already in the presence of the shortest alcohol studied (C8OH): A_{UC} = 71.6 ± 0.9 Å^2; for longer alcohols further increase of A_{UC} was observed, with a maximal value A_{UC} = 74.8 ± 0.8 Å^2 obtained for C18OH (not shown). Jørgensen et al. [51] concluded from the computer-simulation studies that the presence of foreign molecules in the bilayer leads to an increase in the fractional membrane area associated with the interfacial region. As discussed in more detail by Löbbecke and Cevc [52], the presence of alcohol OH group in the headgroup region increases the effective lipid headgroup volume and induces a lateral expansion in the interfacial region. Our results are in agreement with these conclusions and allow quantifying this lateral expansion. Following the concept of mean partial molecular interfacial areas in bilayers discussed extensively by Edholm and Nagle [53] and the definition of A_{UC} earlier, the bilayer surface area can be expressed as $n_{PCPS} \cdot A_{UC} = n_{PCPS} \cdot \overline{A}_{PCPS} + n_{CnOH} \cdot \overline{A}_{CnOH}$, where $\overline{A}_{PCPS}$ is the partial molecular interfacial area of PCPS, and $\overline{A}_{CnOH}$ that of CnOH. It is seen that the A_{UC} vs. n_{CnOH}:n_{PCPS} data in Figs. 2 and 3 can be satisfactorily fitted by linear functions (r^2 = 0.998), i.e. the partial interfacial areas $\overline{A}_{PCPS}$ and $\overline{A}_{CnOH}$ are most probably constant in the range of n_{CnOH}:n_{PCPS} molar ratios investigated. From the error weighted linear fits we obtained $\overline{A}_{PCPS}$ = 64.62–64.85 Å^2 with the fitting error ≤ | ±0.17 | Å^2, i.e. the same value as A_{PCPS} = 64.6 ± 0.7 Å^2 in the control PCPS sample without CnOH. The partial surface area $\overline{A}_{CnOH}$ was found to increase with the CnOH alkyl chain length n: $\overline{A}_{C8OH}$ = 14.2 ± 0.3 Å^2, $\overline{A}_{C12OH}$ = 19.8 ± 0.5 Å^2 and $\overline{A}_{C18OH}$ = 22.6 ± 0.6 Å^2. These partial interfacial area values are compared in Fig. 4 with apparent molecular interfacial areas A_{CnOH} calculated from A_{UC} data at n_{CnOH}:n_{PCPS} = 0.4 molar ratios simply as $A_{CnOH} = (A_{UC} - A_{PCPS}) n_{PCPS}/n_{CnOH}$. It is seen that $\overline{A}_{CnOH} = A_{CnOH}$ within error margins. It is also seen that the molecular CnOH interfacial area in PCPS bilayers increases with the CnOH alkyl length linearly (r^2 = 0.98): from the error weighted linear fit we obtained A_{CnOH} = (6.9 ± 0.9) + (1.05 ± 0.06) · n in Å^2. The values A_{CnOH} ≤ 20 Å^2 are surprisingly low — the mean surface area 18.8 Å^2 is typical for crystalline states of alkanes and ~20 Å^2 for solid rotator phase of alkanes [54]. We suppose that this

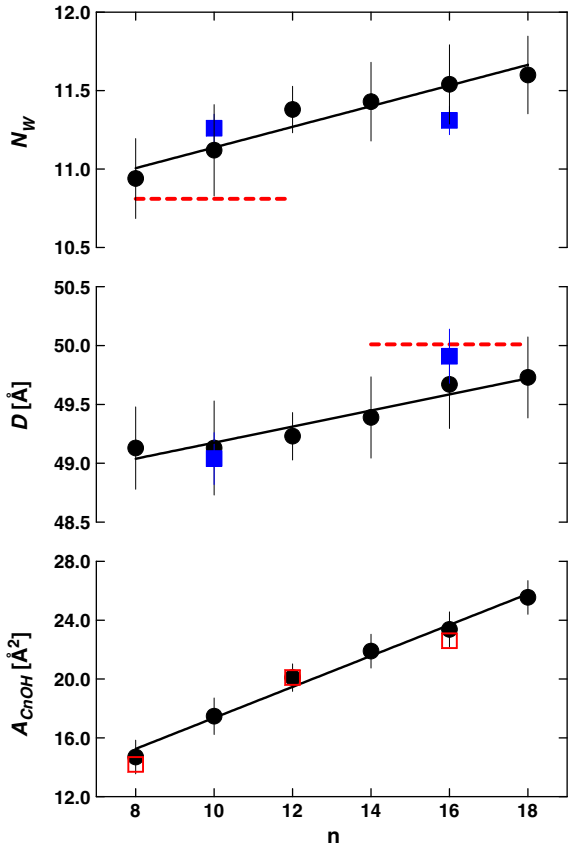

Fig. 4. Molecular CnOH interfacial area (A_{CnOH}), bilayer thickness (D) and number of water molecules (N_W) as a function of the carbon number n in the CnOH chain at n_{CnOH}: n_{PCPS} = 0.4 molar ratio at 20 °C. Dashed lines denote the respective parameter value for the control PCPS bilayers. Contrast variation results — ■, apparent molecular area — ●, partial molecular area — □.

is due to the lipid headgroup: its interfacial area A_{PCPS} is equal or larger than the sum of the areas of the hydrocarbon chain cross-sections, so that a small OH group of CnOH is located underneath at the lipid glycerol

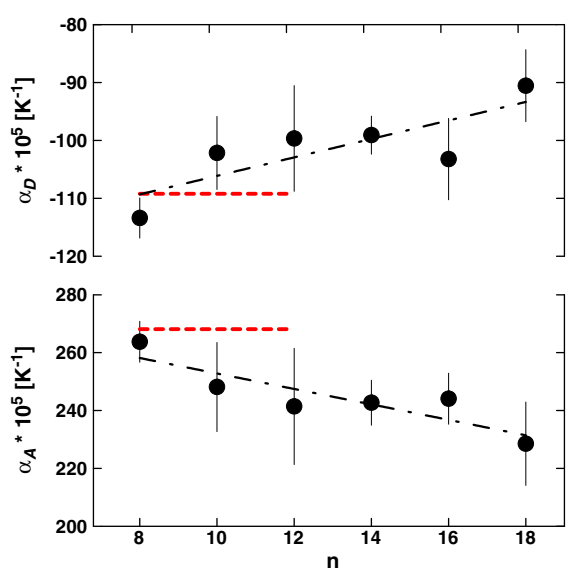

Fig. 5. The coefficients of lateral (α_A) and transversal (α_D) isobaric thermal expansivity of PCPS + CnOH bilayers as a function of the carbon number n in the alcohol chain at CnOH:PCPS = 0.4 molar ratio. Dashed lines denote the respective coefficients of the reference PCPS bilayers.

fragment — similarly to the umbrella model proposed for cholesterol in phospholipid bilayers [55]. In case of cholesterol, the mean molecular area determined by surface pressure measurements on pure cholesterol monolayers was 39 Å^2 [56]. After incorporation of cholesterol into monounsaturated bilayers in unilamellar vesicles a decrease of partial surface area to $\bar{A}_{Chol}$ = 24 Å was observed by SANS [57].

The PCPS + CnOH samples prepared in heavy water at a single contrast were measured further at several temperatures between 20 and 51 °C. All studied parameters, A_{UC}, D and N_w, showed at these temperatures tendencies similar to that found at 20 °C, which is demonstrated in Figs. 3 and 4. In the presence of all studied alcohols the area of unit cell and number of water molecules were found to increase with temperature, while bilayer thickness was decreasing (data not shown). This is attributed, in general, to a continuous formation of *trans-gauche* rotamers within the hydrocarbon chains. Concomitantly, a decrease of the bilayer thickness and increase of the bilayer surface area arises from increased hydrocarbon chain mobility. These changes enhance fluctuations of the lipid bilayer that are accompanied by an intercalation of water molecules from the bulk water phase into the bilayer polar region.

Fig. 5 shows the expansivity coefficients evaluated from experimental data as a function of the carbon number in the alcohol chain. For the reference PCPS system a lateral expansivity coefficient $\alpha_A = (268 \pm 42) \cdot 10^{-5}\,K^{-1}$ was obtained, close to $\alpha_A = 290 \cdot 10^{-5}\,K^{-1}$ found in pure DOPC bilayers by Pan et al. [49]. In the presence of C8OH, α_A was not significantly changed, but it was decreasing as a function of the alcohol chain length reaching the minimum value for C18OH, $\alpha_A = (229 \pm 14) \cdot 10^{-5}\,K^{-1}$. The isobaric transversal expansivity coefficient of the PCPS system was $\alpha_D = -(109 \pm 16) \cdot 10^{-5}\,K^{-1}$, what agrees well with $\alpha_D = -(100 \pm 2) \cdot 10^{-5}\,K^{-1}$ found previously for pure DOPC by SAXD [58]. C8OH decreased slightly the transversal expansivity of the bilayer, while longer alcohols increased it. Maximal increase was observed in the presence of C18OH, $\alpha_D = -(90.5 \pm 6.2) \cdot 10^{-5}\,K^{-1}$. It follows that the effect of alcohols on the thermal behavior of the bilayer depends significantly on the alcohol chain length — longer alcohols stabilize the bilayer against the temperature effects more than short alcohols.

3.3. 3.3. Coarse-grained molecular simulations

Starting from initial configurations in which a number of lipids from the PC bilayer were randomly replaced by alcohol molecules, the systems quickly equilibrate. The alcohols diffuse mainly laterally inside one of the two leaflets, but they are also able to cross the hydrophobic core of the bilayer by a flip-flop mechanism. The residence time of the alcohols inside a leaflet was found to be of the order of 600 ns, with only a small dependency on alcohol chain length and concentration. Only a small fraction of the C8OH molecules have been observed occasionally entering the water phase and subsequently returning into the membrane. Representative snapshots from the simulations are shown in Fig. 6. No segregation is observed to occur between the alcohols and the lipids, in line with the results from our experiments at the studied concentration (0.4 CnOH molar ratio in the bilayer).

In all of the systems, the alcohol molecules are preferentially positioned with their polar headgroups embedded in the lipid headgroup region, close to the glycerol moieties, while their chains are configured similarly to the lipid chains. The exact location of the alcohol headgroups is depicted in red in Fig. 7, in which the partial densities of glycerol, choline and phosphate beads are shown for the pure DOPC membrane (dashed lines) and for the PC bilayer with octanol incorporated (solid lines). The alcohol insertion in the bilayer reduces the distance between any two similar peaks in the figure, decreasing thus the membrane thickness.

The computed values of the membrane thickness are reported in Table 2. The simulation data reflect the distance between the two

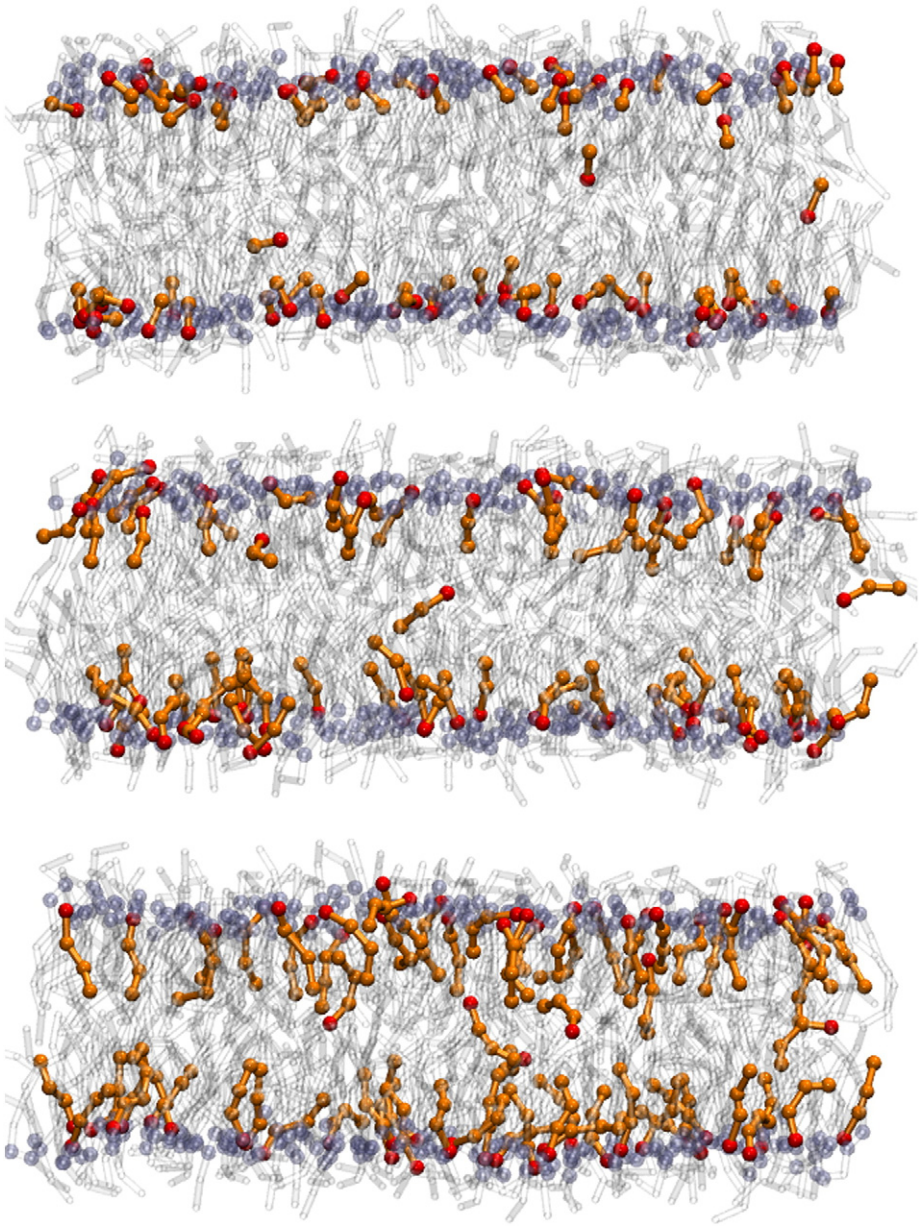

Fig. 6. Snapshots of a PC bilayer incorporating C8OH (top), C12OH (center) and C16OH (bottom) at CnOH: PC = 0.4 molar ratio. The alcohol is represented in red for the head and orange for the chain. The lipids are depicted in transparent blue with their glycerol moieties represented as beads. The water particles are not shown for clarity.

maxima in the phosphate distributions D_{PP} (green curves from Fig. 7), whereas the SANS data are defined as the sum of polar and hydrophobic regions thicknesses. Due to this difference, a quantitative comparison cannot be done between the experimental and computational thickness values, but, more importantly, the same trends are observed after alcohol incorporation. D_{PP} of the bilayer containing C8OH is smaller in comparison with the one of the pure lipid bilayer. When alcohols with longer chains are incorporated, D_{PP} increases back to the thickness of the pure bilayer.

In an attempt to separately estimate the thickness of the polar and the hydrophobic regions we have calculated the partial density (perpendicular to the membrane plane) of all the choline and phosphate beads from one leaflet (Fig. 8A), and of the lipid chain beads (Fig. 8B). For all types of alcohols included in the bilayer, a decrease is observed in the width of the distribution of the lipid polar headgroups, as for the experimental measured D_H, but the length dependence of this decrease is not evident from the MD data. In Fig. 8B, the density of the lipid chain beads is plotted, separately for the two leaflets. When C8OH molecules are present in the bilayer, the total width of the two leaflet distributions decreases compared to pure PC — an effect amplified with increasing alcohol concentration (data not shown). At the concentrations employed in this study no interdigitation of the chains from the two monolayers took place, as illustrated in the central, overlapping part of the distributions. The thickness decrease is less evident when C12OH and C16OH are considered. Since their chains are longer, they do not create as much extra space, to be filled by the lipid acyl chains, as the C8OH molecules do.

The alcohol insertion in the bilayer also generates more space for the lipid headgroups and the area per lipid consequently increases. Our calculated values for the A (gathered in Table 2) are in excellent qualitative agreement with the reported experimental A_{UC} values (cf. Fig. 3). The area increases both with the alcohol concentration and with the alcohol chain length. Table 2 includes also the mean partial

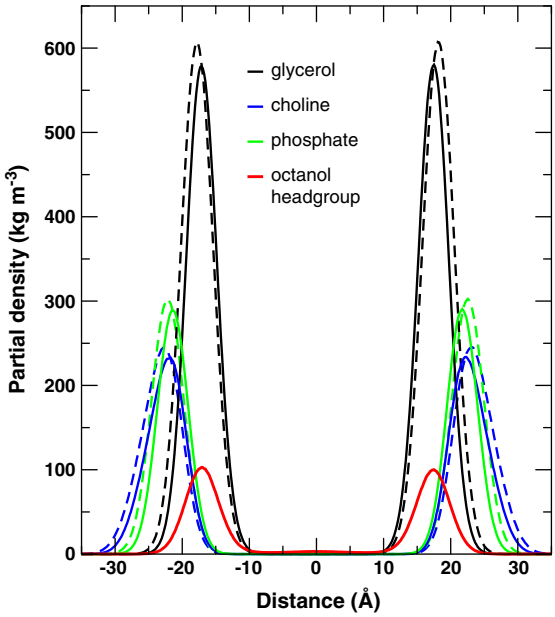

Fig. 7. The partial density distributions of the glycerol (black), choline (blue), phosphate (green) and alcohol headgroups (red) in the direction perpendicular to the bilayer plane. The dashed lines correspond to the pure PC bilayer and the solid lines to n_{C8OH}:n_{PC} = 0.4 molar ratio. The center of the membrane is located at 0 Å.

interfacial areas of the alcohols A_A calculated using Eq. (8). This area follows the same trends as the area per lipid when alcohol concentration or chain length is varied. As in the experimental work, the values obtained from the MD simulations are very small compared with the area per alcohol in the pure crystalline phase. Such discrepancy may have two reasons: (i) the localization of the alcohol headgroups under the lipid headgroups, making them only partially visible in the experiments (umbrella model); (ii) the alcohol flip-flop in-between the leaflets, making the effective number of alcohol molecules in one leaflet smaller than estimated. Concerning the second possibility, from the density distribution (cf. Fig. 7) we have estimated that, on average, only about 3% of the alcohol molecules are located in the middle of the bilayer during the simulation. This may cause a slight underestimation of their partial area, but not enough to account for the difference with respect to the area of crystalline alcohols. The umbrella model therefore seems to be in place.

To shed more light on the effect of alcohols at the molecular level, we have computed the order parameter S of all the bonds along the lipid chains. The obtained order parameters for the lipid bonds are compared in Fig. 9 for the systems at CnOH:DOPC = 0.4 molar ratio. An additional case for C8OH at 2.0 molar ratio is included to emphasize the observed trend. The alcohols increase the order

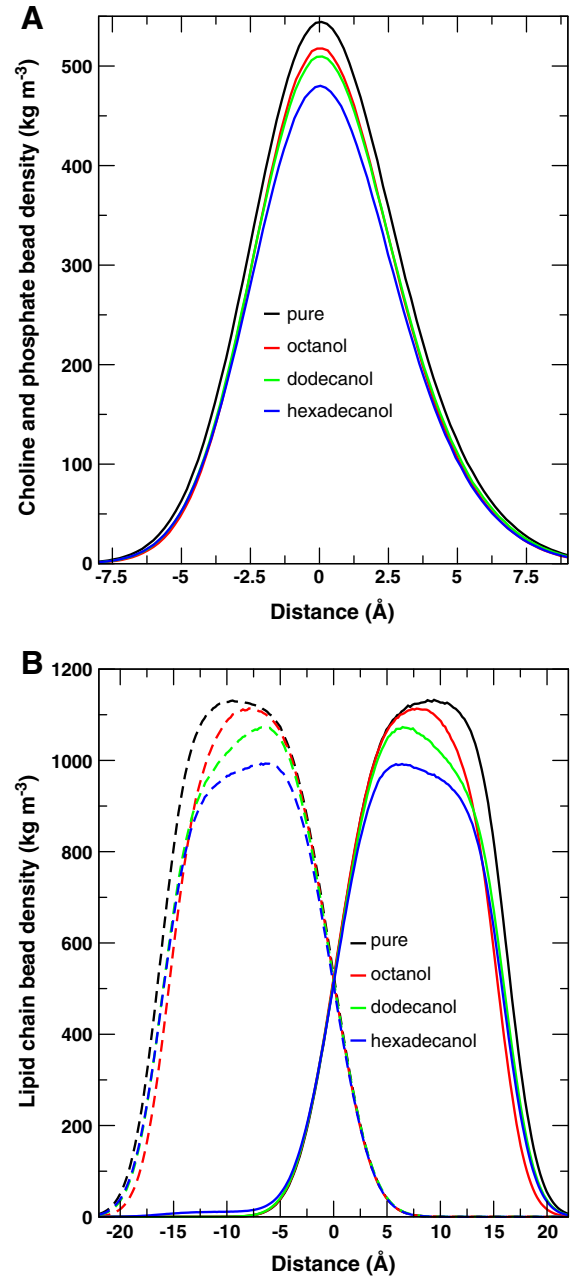

Fig. 8. The partial density distributions of all the choline and phosphate beads form one membrane leaflet (A) and for the lipid chain beads (B) for a pure PC membrane (black) and PC with C8OH (red), C12OH (green) and C16OH (blue) at n_{CnOH}:n_{PC} = 0.4 molar ratio. In panel B) the distributions are computed separately for the upper (solid lines) and lower leaflet (dashed lines).

Table 2
Structural properties (area per lipid — A, alcohol partial surface area — A_A, distance between the two maxima in the phosphate distributions — D_{PP}) of simulated PC bilayers and bilayer thickness D obtained by SANS at different alcohol concentrations and alcohol chain lengths. The error estimates of A, A_A and D_{PP} report the standard errors obtained from splitting the trajectory into ten sub-intervals, which were checked to be uncorrelated.

System	n_{CnOH}:n_{DOPC}	A [Å2]	A_A [Å2]	D_{PP} [Å]	D [Å]
DOPC	0	66.12 ± 0.01	–	44.86 ± 0.66	50.01 ± 0.32
DOPC + C8OH	0.2	68.51 ± 0.01	11.95 ± 0.01	44.30 ± 0.46	49.50 ± 0.12
DOPC + C12OH	0.2	69.41 ± 0.01	16.45 ± 0.01	44.51 ± 0.31	49.58 ± 0.34
DOPC + C16OH	0.2	70.49 ± 0.02	21.85 ± 0.02	44.62 ± 0.38	49.94 ± 0.34
DOPC + C8OH	0.4	71.13 ± 0.04	12.52 ± 0.04	43.45 ± 0.44	49.13 ± 0.35
DOPC + C12OH	0.4	72.83 ± 0.04	16.78 ± 0.04	44.27 ± 0.46	49.23 ± 0.20
DOPC + C16OH	0.4	74.97 ± 0.03	22.12 ± 0.03	44.42 ± 0.29	49.67 ± 0.37

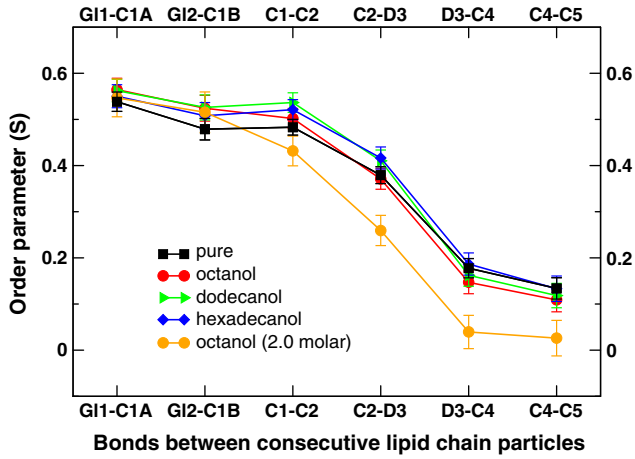

Fig. 9. Order parameter S of lipid chain bonds with respect to bilayer normal. Data are averaged over both chains. The n_{CnOH}:n_{PC} molar ratio is 0.4 if not otherwise indicated.

parameter S of the lipid chain bonds near the lipid headgroups and decrease or unaffect it at their ends. The separation between these two differently affected regions depends on the mismatch between the alcohol and lipid chain lengths. This behavior is in good agreement with the results for the order parameter obtained for DMPC and C8OH by NMR experiments of Pope and Dubro [59]. C8OH increases only the order parameter of the chains near the glycerol region (GL–C1 bonds) since the C8OH molecules are mainly located in this region. The rest of the lipid chains have more free space to fill and even to kink back from the bilayer center (S decreases). Consequently, the bilayer thickness decreases compared with pure DOPC. At the other limit, C16OH molecules, while also creating additional space in the headgroup region, increase the order parameters almost along the entire lipid chain. Therefore the hydrophobic thickness increases, explaining the overall increase in the total membrane thickness compared to the bilayer with C8OH.

4. Conclusions

Outer $^2H_2O/H_2O$ contrast variation experiments showed, that the polar region thickness D_H of fluid DOPC + DOPS + CnOH bilayers decreases as a function of alkyl chain length and CnOH:PCPS molar ratio. In following experiments at single 100% ^2H_2O contrast we found, that the bilayer thickness D decreases with increasing CnOH:PCPS molar ratio from initial 50 ± 0.3 Å (at 20 °C) for pure lipid bilayer, and increases with increasing CnOH chain length at fixed 0.4 molar ratio. The CnOH effect on the bilayer thickness can be explained by the mismatch between CnOH and PCPS hydrocarbon chain lengths, as confirmed with coarse-grained MD simulations, where all CnOHs studied were found to increase the order parameter of the lipid chains near the lipid headgroups and decrease or unaffect it at their ends, depending on CnOH chain length.

Our results can be well interpreted in connection with the cut-off effect observed for anesthetic and biocidal potencies of CnOHs. To evaluate the effect of the CnOHs actually located in the bilayer, one has to take into account the partition coefficient K_p of the studied CnOHs. K_p exponentially increases with CnOH chain length from $K_p \sim 1.4 \cdot 10^4$ for C8OH up to $K_p \sim 1.0 \cdot 10^{10}$ for C18OH [3,25,26]. Thus, at a constant CnOH concentration in the sample one would get instead of linearly increasing dependence of D on n a cut-off type dependence with an extreme at intermediate chain length. Therefore, we can suggest, that the CnOH chain length dependent changes in the membrane bilayer thickness could also play a role in their anesthetic and biocidal activities.

Lateral area of the unit cell A_{UC} is significantly increased from initial 64.6 ± 0.7Å^2 (at 20 °C) already in the presence of C8OH at 0.4 molar ratio; further increase is observed with longer CnOHs and at higher molar ratios. Hereby, the partial surface area A_{CnOH} of alcohol molecules in PCPS bilayer was found to linearly increase with the alkyl chain length. The partial interfacial area $A_{CnOH} \leq 20$Å^2 obtained for CnOHs with $n \leq 10$ is surprisingly low, as the mean surface area 18.8 Å^2 is typical for crystalline states of alkanes and ~20 Å^2 for solid rotator phase of alkanes. From the biological point of view it seems to be interesting, that this anomaly appears with CnOHs which have anesthetic and biocidal acivities and therefore might be also connected with the cut-off effect discussed in the Introduction. The experimental trends of D, A_{UC} and A_{CnOH} observed were reproduced with MD simulations of PC bilayers with alcohol molecules inserted. Simulations further showed that the alcohols are preferentially positioned with their OH groups embedded close to the glycerol moieties of the lipid headgroups. According to this, we suppose that the anomaly in A_{CnOH} is caused by the lipid headgroup, which interfacial area is larger or equal comparing to the sum of hydrocarbon chains cross-section areas, so that a small alcohol OH group is located underneath at the lipid glycerol fragment, in analogy to the "umbrella" model suggested for cholesterol location in bilayers.

With increasing temperature, the area of the unit cell A_{UC} and the number of water molecules N_W per phospholipid in the headgroup region were found to increase, whereas the bilayer thickness decreases. Coefficient of lateral expansivity, $\alpha_A = (268 \pm 42) \cdot 10^{-5} K^{-1}$ found for pure lipid bilayer, decreases in CnOH chain length dependent manner. On the other hand, the coefficient of transversal expansivity, $\alpha_D = -(109 \pm 16) \cdot 10^{-5} K^{-1}$ for pure lipid bilayer, is decreased in the presence of C8OH and increased in the presence of longer CnOHs. This suggests that longer CnOHs stabilize the bilayer to the temperature effects more than short CnOHs.

Acknowledgements

This work was supported by the VEGA 1/0295/08 and 1/0159/11 grants and by the JINR project 07-4-1069-09/2011. The SANS experiments were supported by the European Commission under the 7th Framework Programme through the "Research Infrastructures" action of the "Capacities" Programme, Contract No: CP-CSA_INFRA-2008-1.1.1 Number 226507-NMI3. MK thanks Dr. Jana Gallová for valuable discussions and Professor Peter Westh for help with densitometric data evaluation. We are grateful for the computing time allocated by the Netherlands Computing Facilities (NCF) to perform part of the calculations presented in this paper.

References

[1] K.H. Meyer, H. Hemmi, Beiträge zur Theorie der Narkose III, Biochem. Z. 277 (1935) 39–72.
[2] M.J. Pringle, K.B. Brown, K.W. Miller, Can the lipid theories of anesthesia account for the cutoff in anesthetic potency in homologous series of alcohols? Mol. Pharmacol. 19 (1981) 49–55.
[3] N.P. Franks, W.R. Lieb, Partitioning of long-chain alcohols into lipid bilayers: implications for mechanisms of general anesthesia, Proc. Natl. Acad. Sci. USA 83 (1986) 5116–5120.
[4] G.D. Veith, D.J. Call, L.T. Brooke, Structure–toxicity relationships for the fathead minnow, *Pimephales promelas*: narcotic industrial chemicals, Can. J. Fish Aquat. Sci. 40 (1983) 743–748.
[5] C.N. Huhtanen, Inhibition of *Clostridium botulinum* by spice extracts and aliphatic alcohols, J. Food Prot. 43 (1980) 195–196.
[6] I. Kubo, H. Muroi, A. Kubo, Structural functions of antimicrobial long-chain alcohols and phenols, Bioorg. Med. Chem. 3 (1995) 873–880.
[7] T.W. Schultz, L.M. Arnold, T.S. Wilke, M.P. Moulton, Relationships of quantitative structure–activity for normal aliphatic alcohols, Ecotoxicol. Environ. Saf. 19 (1990) 247–253.
[8] D.G. Hammond, I. Kubo, Structure–activity relationship of alkanols as mosquito larvicides with novel findings regarding their mode of action, Bioorg. Med. Chem. 7 (1999) 271–278.

[9] S. Andega, N. Kanikkannan, M. Singh, Comparison of the effect of fatty alcohols on the permeation of melatonin between porcine and human skin, J. Control. Release 77 (2001) 17–25.
[10] K. Vavrova, J. Zbytovska, A. Hrabalek, Amphiphilic transdermal permeation enhancers: structure–activity relationships, Curr. Med. Chem. 12 (2005) 2273–2291.
[11] P.T. Frangopol, D. Mihailescu, Interactions of some local anesthetics and alcohols with membranes, Colloids Surf. B Biointerfaces 22 (2001) 3–22.
[12] P.W. Westerman, J.M. Pope, N. Phonphok, J.W. Doane, D.W. Dubro, The interaction of n-alkanols with lipid bilayer membranes: a 2H-NMR study, Biochim. Biophys. Acta 939 (1988) 64–78.
[13] G.B. Zavoico, L. Chandler, H. Kutchai, Perturbation of egg phosphatidylcholine and dipalmitoylphosphatidylcholine multilamellar vesicles by n-alkanols. A fluorescent probe study, Biochim. Biophys. Acta 812 (1985) 299–312.
[14] H.V. Ly, M.L. Longo, The influence of short-chain alcohols on interfacial tension, mechanical properties, area/molecule, and permeability of fluid lipid bilayers, Biophys. J. 87 (2004) 1013–1033.
[15] B. Griepernau, S. Leis, M.F. Schneider, M. Sikor, D. Steppich, R.A. Bockmann, 1-Alkanols and membranes: a story of attraction, Biochim. Biophys. Acta 1768 (2007) 2899–2913.
[16] L.I. Horvath, J. Cirák, L. Vigh, Relation or Raman order parameters to spin labeling parameters, Chem. Phys. Lipids 27 (1980) 237–250.
[17] N.P. Franks, W.R. Lieb, Molecular and cellular mechanisms of general anaesthesia, Nature 367 (1994) 607–614.
[18] R.S. Cantor, Membrane lateral pressures: a physical mechanism of general anesthesia, Biophys. J. 72 (1997) MPO98.
[19] R.S. Cantor, Breaking the Meyer–Overton rule: predicted effects of varying stiffness and interfacial activity on the intrinsic potency of anesthetics, Biophys. J. 80 (2001) 503A.
[20] S.A. Simon, T.J. McIntosh, Interdigitated hydrocarbon chain packing causes the biphasic transition behavior in lipid/alcohol suspensions, Biochim. Biophys. Acta 773 (1984) 169–172.
[21] T. Adachi, H. Takahashi, K. Ohki, I. Hatta, Interdigitated structure of phospholipid–alcohol systems studied by X-ray diffraction, Biophys. J. 68 (1995) 1850–1855.
[22] J.M. Pope, L. Walker, D.W. Dubro, On the ordering of *N*-alkane and *N*-alcohol solutes in phospholipid bilayer model membrane systems, Chem. Phys. Lipids 35 (1984) 259–277.
[23] V.I. Petrenko, M. Klacsová, A.I. Beskrovnyy, D. Uhríková, P. Balgavý, Interaction of long-chain *n*-alcohols with fluid DOPC bilayers: a neutron diffraction study, Gen. Physiol. Biophys. 29 (2010) 355–361.
[24] N. Kučerka, J. Pencer, J.N. Sachs, J.F. Nagle, J. Katsaras, Curvature effect on the structure of phospholipid bilayers, Langmuir 23 (2007) 1292–1299.
[25] E.S. Rowe, F. Zhang, T.W. Leung, J.S. Parr, P.T. Guy, Thermodynamics of membrane partitioning for a series of n-alcohols determined by titration calorimetry: role of hydrophobic effects, Biochemistry 37 (1998) 2430–2440.
[26] T.H. Aagaard, M.N. Kristensen, P. Westh, Packing properties of 1-alkanols and alkanes in a phospholipid membrane, Biophys. Chem. 119 (2006) 61–68.
[27] G5-4 Small Angle Neutron Scattering Facility PAXE, Laboratoire Léon Brillouin (CEA-CNRS), CEA-Saclay, 91191 Gif-sur-Yvette Cedex, France, 1995, http://www-llb.cea.fr/spectros/spectro/g5-4.html. Laboratoire Léon Brillouin (CEA-CNRS), CEA-Saclay. 1995. 16-3-2010.
[28] N. Kučerka, D. Uhríková, J. Teixeira, P. Balgavý, Lipid bilayer thickness in extruded liposomes prepared from 1,2-diacylphosphatidylcholines with monounsatured acyl chains: a small-angle neutron scattering study, http://www.fpharm.uniba.sk/fileadmin/user_upload/admin/Acta_facultatis/Tomus_L/Kucerka__Uhrikova__Balgavy.PDF, Acta Facult. Pharm. Univ. Comenianae 50 (2003) 78–89.
[29] J. Gallová, D. Uhríková, N. Kučerka, J. Teixeira, P. Balgavý, Hydrophobic thickness, lipid surface area and polar region hydration in monounsaturated diacylphosphatidylcholine bilayers: SANS study of effects of cholesterol and beta-sitosterol in unilamellar vesicles, Biochim. Biophys. Acta 1778 (2008) 2627–2632.
[30] D. Uhríková, N. Kučerka, J. Teixeira, V.I. Gordeliy, P. Balgavý, Structural changes in dipalmitoylphosphatidylcholine bilayer promoted by Ca^{2+} ions: a small-angle neutron scattering study, Chem. Phys. Lipids 155 (2008) 80–89.
[31] M. Klacsová, P. Westh, P. Balgavý, Molecular and component volumes of saturated *n*-alkanols in DOPC + DOPS bilayers, Chem. Phys. Lipids 163 (2010) 498–505.
[32] D. Uhríková, P. Rybár, T. Hianik, P. Balgavý, Component volumes of unsaturated phosphatidylcholines in fluid bilayers: a densitometric study, Chem. Phys. Lipids 145 (2007) 97–105.
[33] R.C. Weast, Handbook of Chemistry and Physics, The Chemical Rubber Co., Cleveland, 1969.
[34] V.F. Sears, Neutron scattering lengths and cross-sections, in: K. Skold, D.L. Price (Eds.), Methods in Experimental Physics, vol. 23, Academic Press, New York, 1986, pp. 521–550.
[35] N. Kučerka, J. Gallová, D. Uhríková, P. Balgavý, M. Bulacu, S.J. Marrink, J. Katsaras, Areas of monounsaturated phosphatidylcholines, Biophys. J. 97 (2009) 1926–1932.
[36] B. Hess, C. Kutzner, D. Van Der Spoel, E. Lindahl, GROMACS 4: algorithms for highly efficient, load-balanced, and scalable molecular simulation, J. Chem. Theory Comput. 4 (2008) 435–447.
[37] S.J. Marrink, H.J. Risselada, S. Yefimov, D.P. Tieleman, A.H. de Vries, The MARTINI force field: coarse grained model for biomolecular simulations, J. Phys. Chem. B 111 (2007) 7812–7824.
[38] S.J. Marrink, A.H. de Vries, A.E. Mark, Coarse grained model for semiquantitative lipid simulations, J. Phys. Chem. B 108 (2004) 750–760.
[39] A.N. Dickey, R. Faller, Investigating interactions of biomembranes and alcohols: a multiscale approach, J. Polym. Sci. B 43 (2005) 1025–1032.
[40] N.D. Winter, G.C. Schatz, Coarse-grained molecular dynamics study of permeability enhancement in DPPC bilayers by incorporation of lysolipid, J. Phys. Chem. B 114 (2010) 5053–5060.
[41] M. Kranenburg, B. Smit, Simulating the effect of alcohol on the structure of a membrane, FEBS Lett. 568 (2004) 15–18.
[42] H.J.C. Berendsen, J.P.M. Postma, W.F. van Gunsteren, A. DiNola, J.R. Haak, Molecular dynamics with coupling to an external bath, J. Chem. Phys. 81 (1984) 3684–3690.
[43] T. Nawroth, H. Conrad, K. Dose, Neutron small angle scattering of liposomes in the presence of detergents, Physica B 156&157 (1989) 477–480.
[44] W.J. Sun, R.M. Suter, M.A. Knewtson, C.R. Worthington, S. Tristram-Nagle, R. Zhang, J.F. Nagle, Order and disorder in fully hydrated unoriented bilayers of gel phase DPPC, Phys. Rev. E 49 (1994) 4665–4676.
[45] S. Tristram-Nagle, Y. Liu, J. Legleiter, J.F. Nagle, Structure of gel phase DMPC determined by X-ray diffraction, Biophys. J. 83 (2002) 3324–3335.
[46] G. Pabst, M. Rappolt, H. Amenitsch, P. Laggner, Structural information from multilamellar liposomes at full hydration: full q-range fitting with high quality X-ray data, Phys. Rev. E. 62 (2000) 4000–4009.
[47] G. Büldt, H.U. Gally, J. Seelig, G. Zaccai, Neutron diffraction studies on phosphatidylcholine model membranes. I. Head group conformation, J. Mol. Biol. 134 (1979) 673–691.
[48] G. Zaccai, G. Büldt, A. Seelig, J. Seelig, Neutron diffraction studies on phosphatidylcholine model membranes. II. Chain conformation and segmental disorder, J. Mol. Biol. 134 (1979) 693–706.
[49] J. Pan, S. Tristram-Nagle, N. Kučerka, J.F. Nagle, Temperature dependence of structure, bending rigidity, and bilayer interactions of dioleoylphosphatidylcholine bilayers, Biophys. J. 94 (2008) 117–124.
[50] H.I. Petrache, S. Tristram-Nagle, K. Gawrisch, D. Harries, V.A. Parsegian, J.F. Nagle, Structure and fluctuations of charged phosphatidylserine bilayers in the absence of salt, Biophys. J. 86 (2004) 1574–1586.
[51] K. Jørgensen, J.H. Ipsen, O.G. Mouritsen, D. Bennett, M.J. Zuckermann, The effects of density fluctuations on the partitioning of foreign molecules into lipid bilayers: application to anaesthetics and insecticides, Biochim. Biophys. Acta 1067 (1991) 241–253.
[52] L. Löbbecke, G. Cevc, Effects of short-chain alcohols on the phase behavior and interdigitation of phosphatidylcholine bilayer membranes, Biochim. Biophys. Acta 1237 (1995) 59–69.
[53] O. Edholm, J.F. Nagle, Areas of molecules in membranes consisting of mixtures, Biophys. J. 89 (2005) 1827–1832.
[54] D.M. Small, Lateral chain packing in lipids and membranes, J. Lipid Res. 25 (1984) 1490–1500.
[55] J. Huang, G.W. Feigenson, A microscopic interaction model of maximum solubility of cholesterol in lipid bilayers, Biophys. J. 76 (1999) 2142–2157.
[56] P.A. Hyslop, B. Morel, R.D. Sauerheber, Organization and interaction of cholesterol and phosphatidylcholine in model bilayer membranes, Biochemistry 29 (1990) 1025–1038.
[57] J. Gallová, D. Uhríková, N. Kučerka, J. Teixeira, P. Balgavý, Partial area of cholesterol in monounsaturated diacylphosphatidylcholine bilayers, Chem. Phys. Lipids 163 (2010) 765–770.
[58] D. Uhríková, M. Hanulová, S.S. Funari, R.S. Khusainova, F. Šeršeň, P. Balgavý, The structure of DNA-DOPC aggregates formed in presence of calcium and magnesium ions: a small-angle synchrotron X-ray diffraction study, Biochim. Biophys. Acta 1713 (2005) 15–28.
[59] J.M. Pope, D.W. Dubro, The interaction of n-alkanes and n-alcohols with lipid bilayer membranes: a ^{2}H-NMR study, Biochim. Biophys. Acta 858 (1986) 243–253.